euronoise

Development of a simple and accurate approximation method for the Gaussian beam expansion technique

Wei Liu, Peifeng Ji and Jun Yang

Institute of Acoustics, Chinese Academy of Sciences, Bei-Si-Huan-Xi Road, 100080 Beijing, China
junyang.ioa@gmail.com

The calculation of the sound field can be greatly simplified by using the Gaussian beam expansion technique. The source distribution function is expressed as the superposition of a small number of Gaussian functions, and the expansion coefficients could be obtained by minimizing an object function in the spatial or *k*-space domain. In this paper, a fast algorithm is developed to determine the Gaussian function coefficients for a more accurate approximation. Two-stage procedures are employed in the proposed method. Firstly, two real coefficients are estimated by a simple search approach, and then the least mean square (LMS) algorithm is adopted for determining the optimal expansion coefficients. Finally, the presented method is evaluated in the case of calculation of sound fields radiated from a piston and a rectangular planar source. Simulation results show that, compared with the previous approaches, the developed scheme is simple to implement with high accuracy.

1 Introduction

Recently, the Gaussian beam expansion technique has been applied to the modelling of sound beams [1-8]. An analytical expression can be obtained to predict the sound field radiated from a circular, elliptic or rectangular source. It reduces the computational time and also simplifies the calculation of the second order sound field. The principle of the Gaussian beam expansion technique is to decompose the source distribution function into the superposition of a small number of Gaussian functions. A key problem of this treatment is how to determine the expansion coefficients of Gaussian functions. Wen and Breazeale [1, 2] achieved the expansion coefficients by minimizing the square error between the superposition of Gaussian functions and the velocity distribution on the surface of circular piston. This procedure is performed in the spatial domain, which is named a spatial domain method. Ding *et al.* [4] also proposed a scheme to compute a set of expansion coefficients. On the other hand, Sha *et al.* [5, 6] obtained the expansion coefficients for a rectangular and elliptical planar piston in a two-dimensional spatial Fourier transform (*k*-space) domain. Kim *et al.* [8] reviewed these two methods and demonstrated that there is a simple relationship between the coefficients obtained in the spatial domain and *k*-space domain. It is pointed out that the two sets of coefficients could be transformed each other. However, the existing nonlinear optimization algorithms for computing the coefficients are complicated and time-consuming. This brings the need of an efficient algorithm to obtain the expansion coefficients.

This paper presents a new algorithm to determine the Gaussian expansion coefficients of the source distribution. The 10-term, 15-term and 25-term expansion coefficients are obtained by the proposed method and compared with the corresponding coefficients in Ref. [1, 2, 8]. It is proved that the developed algorithm can provide a higher accurate approximation of the source function. For circular and rectangular transducers, the calculated sound fields by the proposed method agree well with the ones using Fresnel integral, which is superior to the previous approaches. Furthermore, the 25-term expansion coefficients with on-axis matching [2] are provided to improve the calculation of the near field radiated from a circular piston.

2 Theory

The sound field of ultrasonic transducer can be expressed by the Fresnel field integral,

$$p(x,y,z)=\frac{k}{i2\pi z}\int_{-\infty}^{+\infty}\int_{-\infty}^{+\infty}\exp\left(\frac{ik}{2}\frac{(x-x')^2+(y-y')^2}{z}\right)\times V(x',y')\,dx'dy'. \quad (1)$$

The source is in the plane of z=0, $V(x', y')$ is a normalized velocity on the transducer's surface, k is the wave number, (x, y, z) is the field point. Factor $\exp[-i(\omega t-kz)]$ is omitted.

2.1 Circular transducer

Define the dimensionless variables $\rho=\sqrt{x^2+y^2}/r$ and $\sigma=z/z_R$, Eq.(1) becomes the sound field of a circular transducer,

$$p(\rho,\sigma)=\int_0^{+\infty}\frac{2}{i\sigma}\exp\left(i\frac{\rho^2+\rho'^2}{\sigma}\right)J_0\left(\frac{2\rho\rho'}{\sigma}\right)\rho'\times V(\rho')\,d\rho', \quad (2)$$

where r is the radius of the source, $z_R=kr^2/2$ is Rayleigh distance. Using the Gaussian beam expansion technique, the function $V(\rho')$ can be expressed as

$$V(\rho')=\sum_{n=1}^{N}A_n\exp(-B_n\rho'^2), \quad (3)$$

Substituting Eq.(3) into Eq.(2) yields

$$p(\rho,\sigma)=\sum_{n=1}^{N}\frac{A_n}{1+iB_n\sigma}\exp\left(-\frac{B_n\rho^2}{1+iB_n\sigma}\right). \quad (4)$$

2.2 Rectangular transducer

Define the dimensionless variables $\xi=x/\sqrt{ab}$, $\zeta=y/\sqrt{ab}$ and $\eta=2z/kab$, Eq.(1) becomes the sound field of a rectangular transducer,

$$p(\xi,\zeta,\eta)=\frac{1}{i\pi\eta}\int_{-\infty}^{+\infty}\int_{-\infty}^{+\infty}\exp\left(i\frac{(\xi-\xi')^2+(\zeta-\zeta')^2}{\eta}\right)\times V(\xi',\zeta')\,d\xi'd\zeta', \quad (5)$$

where a and b are the half major and half minor axes of the transducer, respectively. For a uniform source, the function $V(\xi',\zeta')$ could be expressed as,

$$V(\xi',\zeta')=\left\{\sum_{n=1}^{N}A_n\exp\left(-B_n\frac{b}{a}\xi'^2\right)\right\}\cdot\left\{\sum_{n=1}^{N}A_n\exp\left(-B_n\frac{a}{b}\zeta'^2\right)\right\}. \quad (6)$$

Substituting Eq.(6) into Eq.(5), we have the Gaussian beam solution in the following [3],

$$p(\xi,\zeta,\eta)=\left[\sum_{n=1}^{N}\frac{A_n}{\sqrt{1+i\eta B_n\, b/a}}\exp\left(-\frac{\xi^2 B_n\, b/a}{1+i\eta B_n\, b/a}\right)\right]\cdot\left[\sum_{n=1}^{N}\frac{A_n}{\sqrt{1+i\eta B_n\, a/b}}\exp\left(-\frac{\zeta^2 B_n\, a/b}{1+i\eta B_n\, a/b}\right)\right]. \quad (7)$$

3 Determination of the Gaussian expansion coefficients

In this section, an alternative algorithm is presented for a fast and accurate computation of the expansion coefficients.

3.1 The new algorithm

The expansion coefficients A_n and B_n are determined by minimizing the object function Q,

$$Q=\int_{-\infty}^{+\infty}\left|V(x)-\sum_{n=1}^{N}A_n\exp(-B_n x^2)\right|^2 dx\,, \quad (8)$$

where the function Q must satisfy the conditions,

$$\partial Q/\partial A_j^*=0,\qquad j=1,2,...N\,. \quad (9)$$

From Eq.(9), we have

$$A=C^{-1}\cdot D\,, \quad (10)$$

where

$$A=\begin{bmatrix}A_1\\ .\\ A_n\\ .\\ A_N\end{bmatrix},\ C=\begin{bmatrix}C_{11} & . & C_{1n} & . & C_{1N}\\ . & . & & & .\\ C_{j1} & & C_{jn} & & C_{jN}\\ . & & & . & .\\ C_{N1} & . & C_{Nn} & . & C_{NN}\end{bmatrix},\ D=\begin{bmatrix}D_1\\ .\\ D_j\\ .\\ D_N\end{bmatrix},$$

$$C_{jn}=\int_{-\infty}^{+\infty}\exp\left[-\left(B_j^*+B_n\right)x^2\right]dx=\sqrt{\pi/\left(B_j^*+B_n\right)}\,,$$

$$D_j=\int_{-\infty}^{+\infty}V(x)\cdot\exp\left(-B_j^* x^2\right)dx\,.$$

Thus coefficients A_n are determined by B_n. Suppose $B_n=\alpha_n-i\beta_n$ and define

$$\alpha_n=\delta,\qquad \beta_n=\frac{2n-1-N}{N-1}k_{\max},\qquad n=1,2,...N\,. \quad (11)$$

Coefficients B_n only depend to two real coefficients δ and $k_{\max}$. Using Eq.(10) and Eq.(11), Q is determined by δ and $k_{\max}$. Therefore, an efficient algorithm is given as following:

First stage: δ and $k_{\max}$ are searched to minimize Q as N is fixed. Empirically, δ is not too large and $k_{\max}$ increases as N grows. An example will be given in section 3.2 to explain the search method.

Second stage: The obtained δ and $k_{\max}$ in first stage are used to compute initial values of coefficients B_n, and then a least mean square (LMS) algorithm is employed to calculate the "optimized" expansion coefficients.

3.2 Example

Consider a source with the following velocity function,

$$V(x)=\begin{cases}1 & |x|\le 1\\ 0 & \text{elsewhere}\end{cases}. \quad (12)$$

The function $V(x)$ can be expressed by the inverse Fourier transform,

$$V(x)=\frac{1}{2\pi}\int_{-\infty}^{+\infty}\frac{2\sin k_x}{k_x}\exp(ik_x x)dk_x\,. \quad (13)$$

Changing x into x^2, Eq.(13) can be written as

$$V(x^2)=V(x)=\frac{1}{2\pi}\int_{-\infty}^{+\infty}\frac{2\sin k_x}{k_x}\exp(ik_x x^2)dk_x\,. \quad (14)$$

Multiplying Eq.(14) by $\exp(-\delta x^2)$ and taking a limit, we have

$$V(x)=\lim_{\delta\to 0+}\frac{1}{2\pi}\int_{-\infty}^{+\infty}\frac{2\sin k_x}{k_x}\exp\left[-(\delta-ik_x)x^2\right]dk_x\,. \quad (15)$$

Right side of Eq.(15) can be written as series,

$$V(x)=\sum_{m=-\infty}^{+\infty}E_m\exp\left[-(\delta-ik_{x,m})x^2\right]. \quad (16)$$

Using Gaussian expansion technique, the function $V(x)$ can be expressed by

$$V(x)=\sum_{n=1}^{N}A_n\exp\left[-(\alpha_n-i\beta_n)x^2\right]. \quad (17)$$

It is clear from Eq.(16) and Eq.(17) that β_n is identical to $k_{x,m}$. Consider β_n as "frequency" item, $k_{x,m}$ increases with m. That is the reason to offer Eq.(11) in section 3.1. The maximum of β_n is $k_{\max}$.

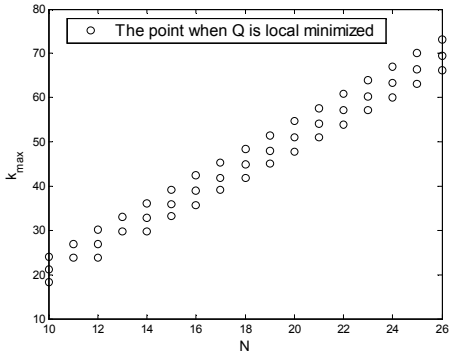

Fig.1 The relationship between N and $k_{\max}$.

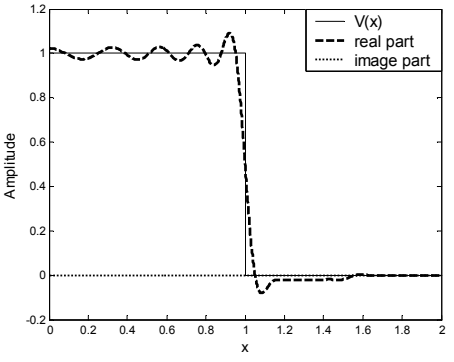

Fig.2 The velocity distribution of a 10-term Gaussian expansion coefficients when δ=2.9, $k_{\max}=6.72\pi$.

n	A_n	B_n
1	-0.0366 + 0.0698i	0.9568 + 22.0499i
2	-0.2880 - 0.1072i	1.8966 + 17.3281i
3	0.0463 - 0.8593i	2.5687 + 12.2845i
4	2.4278 - 0.4273i	3.1522 + 7.1375i
5	-1.6515 + 6.9321i	3.7397 + 2.2497i
6	-1.6515 - 6.9321i	3.7397 - 2.2497i
7	2.4278 + 0.4273i	3.1522 - 7.1375i
8	0.0463 + 0.8593i	2.5687 - 12.2845i
9	-0.2880 + 0.1072i	1.8966 - 17.3281i
10	-0.0366 - 0.0698i	0.9568 - 22.0499i
Q=0.0133666		

Table 1 10-term coefficients for the uniform piston source

n	A_n	B_n
1	-0.0647 - 0.0042i	1.2100 + 35.6867i
2	0.0334 - 0.2398i	2.3108 + 31.3481i
3	0.5113 - 0.0972i	2.8161 + 26.2901i
4	0.5858 + 0.7912i	3.2223 + 21.1344i
5	-0.6908 + 1.5627i	3.4860 + 15.8696i
6	-3.0363 + 0.5081i	3.6537 + 10.4523i
7	-3.6501 - 6.3857i	4.0206 + 5.0002i
8	13.6222	4.3552
9	-3.6501 + 6.3857i	4.0206 - 5.0002i
10	-3.0363 - 0.5081i	3.6537 - 10.4523i
11	-0.6908 - 1.5627i	3.4860 - 15.8696i
12	0.5858 - 0.7912i	3.2223 - 21.1344i
13	0.5113 + 0.0972i	2.8161 - 26.2901i
14	0.0334 + 0.2398i	2.3108 - 31.3481i
15	-0.0647 + 0.0042i	1.2100 - 35.6867i
Q=0.0084602		

Table 2 15-term coefficients for the uniform piston source

n	A_n	B_n
1	0.0250 + 0.0903i	2.7353 + 64.7628i
2	-0.1722 + 0.0417i	2.4159 + 60.8489i
3	-0.2335 - 0.2073i	3.0518 + 55.6123i
4	0.0169 - 0.4669i	3.3108 + 50.1677i
5	0.5003 - 0.4462i	3.5307 + 44.6995i
6	0.9303 + 0.0207i	3.7217 + 39.1628i
7	0.9359 + 0.8547i	3.8727 + 33.5837i
8	0.2283 + 1.7047i	3.9930 + 27.9784i
9	-1.2466 + 2.0209i	4.0952 + 22.3454i
10	-3.1897 + 1.1364i	4.1578 + 16.6841i
11	-5.3844 - 1.7978i	4.2756 + 10.9041i
12	-3.2923 - 12.5813i	4.6409 + 5.2178i
13	22.7593	4.9426
14	-3.2923 + 12.5813i	4.6409 - 5.2178i
15	-5.3844 + 1.7978i	4.2756 - 10.9041i
16	-3.1897 - 1.1364i	4.1578 - 16.6841i
17	-1.2466 - 2.0209i	4.0952 - 22.3454i
18	0.2283 - 1.7047i	3.9930 - 27.9784i
19	0.9359 - 0.8547i	3.8727 - 33.5837i
20	0.9303 - 0.0207i	3.7217 - 39.1628i
21	0.5003 + 0.4462i	3.5307 - 44.6995i
22	0.0169 + 0.4669i	3.3108 - 50.1677i
23	-0.2335 + 0.2073i	3.0518 - 55.6123i
24	-0.1722 - 0.0417i	2.4159 - 60.8489i
25	0.0250 - 0.0903i	2.7353 - 64.7628i
Q=0.0048482		

Table 3 25-term coefficients for the uniform piston source

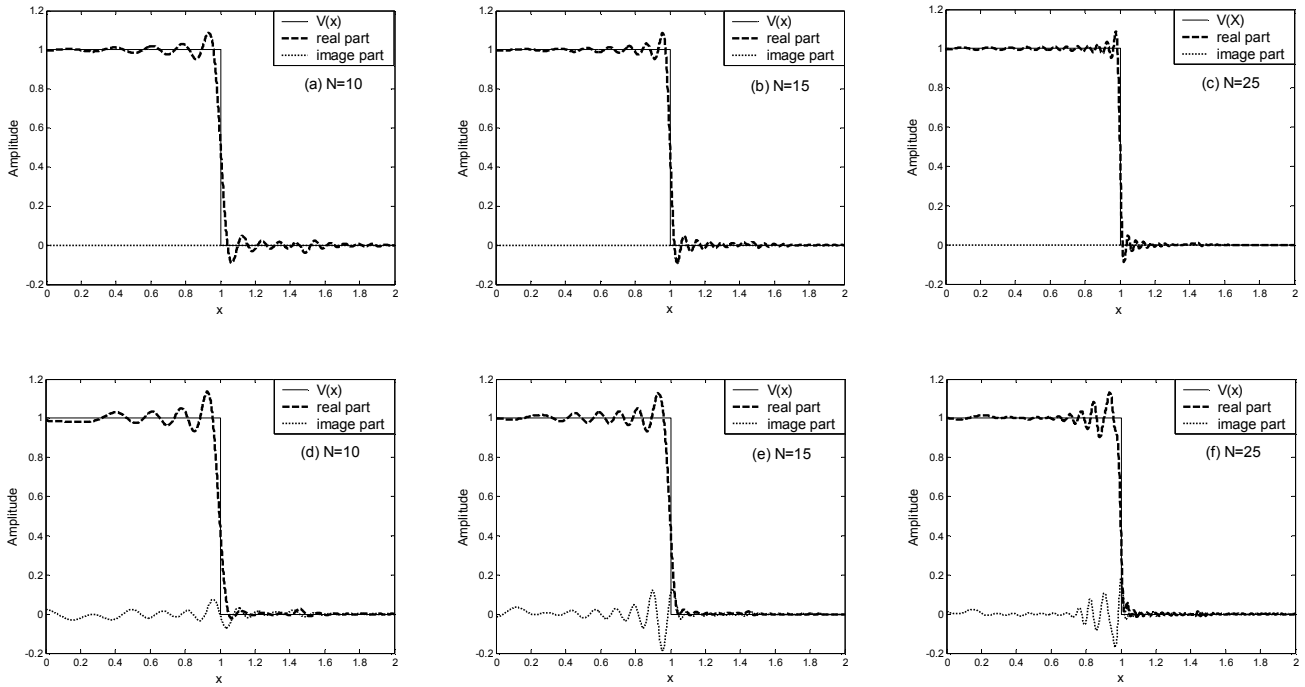

Fig.3 The approximation to the uniform piston source using the two methods: For (a), (b) and (c), the coefficients are from Table 1, 2, and 3; For (d), (e), and (f), the coefficients are given in Ref. [1, 2, 8].

Fig.1 shows the relationship between N and $k_{\max}$ as Q is locally minimized. Obviously, $k_{\max}$ is neither too large nor too small as N is fixed. The bigger N is, the greater $k_{\max}$ is. According to the numerous testing, the value of δ is in the range of 2 and 5. Thus, δ and $k_{\max}$ can be easily determined. Fig.2 shows the real part and image part of the superposition of 10-term Gaussian functions comparing with $V(x)$ when δ=2.9, $k_{\max}$=6.72π and Q=0.0164476.

Next, the LMS algorithm is employed to obtain the optimal expansion coefficients by using δ and $k_{\max}$. The 10-term, 15-term and 25-term coefficients are given in Tables 1, 2 and 3 respectively. Fig.3 illustrates the approximation to the function $V(x)$ using expansion coefficients obtained by proposed method and nonlinear optimization algorithm respectively. The set of coefficients used in Fig.3 (d), (e), (f) are given in Ref. [1, 2, 8]. The corresponding values of Q are 0.0168339, 0.0173398 and 0.0116548, respectively. It is seen from Fig.3 that the presented method approximate $V(x)$ more accurately than the previous approach. Moreover, the obtained coefficients appear in conjugate complex pairs so that the image part of the superposition of Gaussian functions is exactly zero, which has the advantage of computation speed in the algorithm implementation.

4 Simulations

Firstly, in order to demonstrate the validity of the new method, the coefficients in Table 1, 2 and 3 are used in Eq.(4) to calculate the on-axis sound field of the circular transducer with the characteristic value kr=100. Fig.4 shows the sound pressure in the near field ($0.04z_0$< z<$0.18z_0$). It is noted that the Gaussian beam solution agrees well with the Fresnel integral down to distances as small as $0.15z_0$, at which point the N=10 data begin to diverge from the Fresnel integral. The N=15 data down to $0.09z_0$, and the N=25 data down to $0.045z_0$. Fig.5 shows the relative error of on-axis sound pressure between the Fresnel integral and the Gaussian beam solution in the far field (z_0<z<$20z_0$). It can be seen that the relative error is less than 0.45%. The bigger N is, the smaller the relative error is.

Secondly, the 10-term coefficients in Table 1 are compared with the ones given by Wen and Breazeale [1] in the calculation of sound field. Both two sets of coefficients are evaluated in Eq.(8) with the rectangular transducer's ratio b/a=2/3. Fig.6 and Fig.7 show the on-axis sound pressure and relative error in the near field ($0.01Z_0$<z<$0.1Z_0$) and far field (Z_0<z<$10Z_0$), respectively. Obviously, the use of presented 10-term coefficients approximate the Fresnel integral more accurately in near field and has less relative error in far field compared with those given in Ref. [1].

Finally, we improve the new algorithm for the nearfield calculation by introducing a constraint. Although Fresnel integral and the exact sound field (Rayleigh integral) have no distinct difference in far field for ultrasonic wave, they differ from each other in near field. The difference is shown in Fig.8. Because the Gaussian beam solution's limit is Fresnel integral, it is not available to obtain a good nearfield description by minimizing function Q only. Here, we adopt the on-axis matching method [2]. A new set of 25-term expansion coefficients are given in Table 4. Fig.9 shows the 25-term Gaussian beam solution using on-axis matching as a constraint, which is compared with the Rayleigh integral. As shown in Fig.9, the 25-term Gaussian beam solution agrees well with the Rayleigh integral down to distances as small as $0.05z_0$.

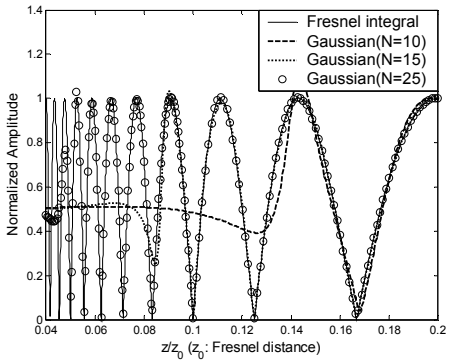

Fig.4 The on-axis near field sound pressure of the circular transducer (with the characteristic value kr=100) calculated by 10-term, 15-term and 25-term Gaussian beam solution.

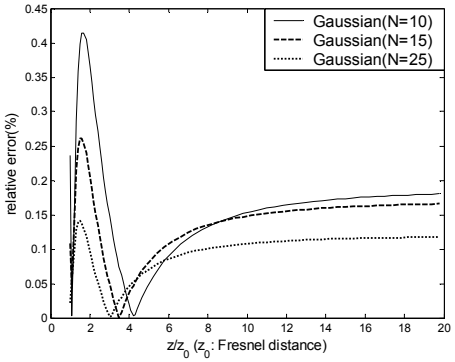

Fig.5 The relative error of the on-axis far field sound pressure of the circular transducer (with the characteristic value kr=100).

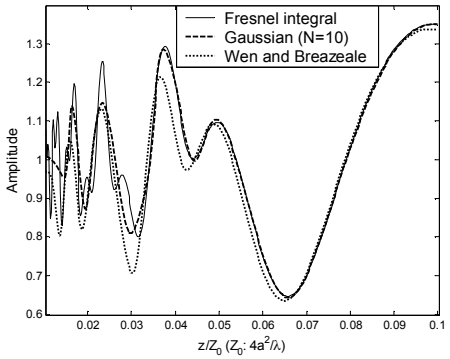

Fig.6 Comparison of the on-axis near field sound pressure of the rectangular transducer, b/a=2/3.

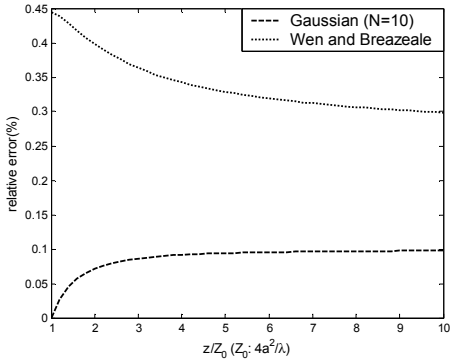

Fig.7 Comparison of the relative error of on-axis far field sound pressure of the rectangular transducer, b/a=2/3.

n	A_n	B_n
1	0.0241 - 0.0155i	2.7372 +64.7861i
2	-0.0408 - 0.0029i	2.5439 +60.8874i
3	0.0964 + 0.0108i	3.1321 +55.4940i
4	-0.1257 - 0.0525i	3.5549 +50.2514i
5	0.3522 - 0.1809i	4.1582 +44.2264i
6	0.2470 + 0.1794i	3.1723 +37.6976i
7	0.2915 - 0.1028i	3.6115 +34.1954i
8	0.6222 + 1.2078i	4.3391 +29.4449i
9	-0.9555 + 2.0721i	4.6465 +23.1049i
10	-3.0511 + 1.2052i	4.4052 +16.9259i
11	-5.2915 - 1.7977i	4.3622 +10.9767i
12	-3.1917 -12.5799i	4.6751 + 5.2243i
13	22.8616 + 0.0240i	4.9578 - 0.0140i
14	-3.1973 +12.6223i	4.6364 - 5.2449i
15	-5.3114 + 1.8505i	4.2523 -10.9256i
16	-3.1415 - 1.0693i	4.1327 -16.6905i
17	-1.2231 - 1.9443i	4.0724 -22.3435i
18	0.2269 - 1.6286i	3.9720 -27.9687i
19	0.9102 - 0.7883i	3.8566 -33.5671i
20	0.8857 + 0.0267i	3.7125 -39.1419i
21	0.4467 + 0.4674i	3.5285 -44.6782i
22	-0.0320 + 0.4605i	3.3130 -50.1472i
23	-0.2645 + 0.1815i	3.0639 -55.5923i
24	-0.1827 - 0.0676i	2.4320 -60.8658i
25	0.0428 - 0.1007i	2.6947 -64.7590i

Table 4 The 25-term expansion coefficients (with on-axis matching) for the uniform piston source

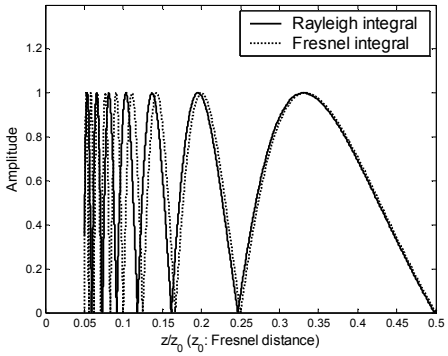

Fig.8 The difference between Rayleigh integral and Fresnel integral of the on-axis near field of the circular transducer (with the characteristic value kr=107.8).

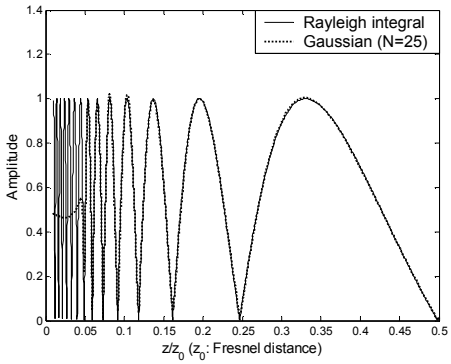

Fig.9 The on-axis near field sound pressure of a 25-term Gaussian beam solution of the circular transducer (with the characteristic value kr=107.8) using the on-axis matching.

5 Conclusion

A new algorithm for determining the Gaussian beam expansion coefficients has been presented. Two-stage procedures are employed to simplify the determination of a set of coefficients. Firstly, two real coefficients are searched to obtain the initial values of exponential coefficients. Secondly, the LMS algorithm is adopted for computing the optimal expansion coefficients. The proposed algorithm has the advantage of providing high approximation accuracy for the sound field calculation with a fast computation. Moreover, the obtained coefficients are conjugate complex pairs and the superposition of Gaussian functions has no image part, which are different from those in the previous approaches. Finally, the on-axis matching method is used to evaluate the nearfield. A high-accuracy approximation is achieved in the near field down to $0.05z_0$, which is unavailable for previous approaches. Simulation results show that our method has significantly improved performance in the calculation of sound field.

References

[1] J. J. Wen, M. A. Breazeale, "A diffraction beam field expressed as the superposition of Gaussian beams", *J. Acoust. Soc. Am.* 83, 1752-1756 (1988)

[2] J. J. Wen, M. A. Breazeale, "Computer optimization of the Gaussian beam description of an ultrasonic field", *Computational Acoustics*. 2, 181-196 (1990)

[3] D. Ding, Y. Zhang, J. Liu, "Some extensions of the Gaussian beam expansion: Radiation fields of rectangular and elliptical transducers", *J. Acoust. Soc. Am.* 113, 3043-3048 (2003)

[4] D. Ding, Y. Zhang, "Notes on the Gaussian beam expansion", *J. Acoust. Soc. Am.* 116, 1401-1405 (2004)

[5] K. Sha, J. Yang, W. S. Gan, "A complex virtual source approach for calculating the diffraction beam field generated by a rectangular planar source", *IEEE Trans. Ultrason. Ferroelectr. Freq. Control.* 50, 890-896 (2003)

[6] J. Yang, K. Sha, W.S. Gan and J. Tian, "Nonlinear wave propagation for a parametric loudspeaker", *IEICE Trans. Fundamentals.* E87-A, 2395-2400 (2004)

[7] J. Yang, K. Sha, W. S. Gan, J. Tian, "Modeling of finite-amplitude sound beams: second order fields generated by a parametric loudspeaker", *IEEE Trans. Ultrason. Ferroelectr. Freq. Control.* 52, 610-618 (2005)

[8] Hak-Joon. Kim, Lester. W. Schmerr, Alexander. Sedov, "Generation of the basis sets for multi-Gaussian ultrasonic beam models—An overview", *J. Acoust. Soc. Am.* 119, 1971-1978 (2006)